REGULAR ARTICLE

Co-localization and unique distributions of two clock proteins CYCLE and CLOCK in the cephalic ganglia of the ground cricket, *Allonemobius allardi*

Qi-Miao Shao · Susumu Hiragaki · Makio Takeda

Abstract CYCLE (CYC) and CLOCK (CLK) are transcriptional activators of the circadian clock genes, *period* (*per*) and *timeless* (*tim*), binding at E-boxes of their upstream regulatory region in *Drosophila*. CYC-like and CLK-like immunohistochemical reactivities (CYC-ir and CLK-ir) were investigated in the ground cricket, *Allonemobius allardi*, in which immunohistochemical reactivities for three circadian clock proteins (PERIOD, Doubletime, and Cryptochrome), two neuropeptides (crustacean cardioactive peptide and diapause hormone), and arylalkylamine-*N*-acetyltransferase had previously been mapped in the brain-subesophageal ganglion (SOG) complex. CYC-ir and CLK-ir occurred predominantly in the cytoplasm of the neurons distributed mainly in the central brain, SOG, and corpora cardiaca. Double-labeling experiments showed that CYC-ir and CLK-ir were co-localized only in the mandibular and maxillary neuromeres of the SOG. The neuronal processes in the dorsolateral region of the protocerebrum partially shared the immunoreactivities, whereas most of the other immunoreactivities were unique. The optic lobe showed reactivity to anti-CYC at small proximal frontodorsal cells and to anti-CLK at small proximal frontoventral cells. The frontal ganglion exhibited CYC-ir in the cell bodies that lacked CLK-ir. No difference in their number, distribution, or staining intensity was found between sampling under light:dark regimes of 16:8 and 12:12. The levels of both CYC-ir and CLK-ir showed no oscillation throughout a 24-h period. The co-localization pattern suggests that the midline cells of the SOG share most of the circadian-related immunoreactivities, thus constituting the heart of the circadian clock in *A. allardi*.

Q.-M. Shao · S. Hiragaki · M. Takeda
Division of Molecular Science,
Graduate School of Science and Technology, Kobe University,
1-1 Rokkodai-cho, Nada-ku, Kobe 657-8501, Japan

M. Takeda (✉)
Graduate School of Science and Technology,
Kobe University,
Nada, Kobe 657-8501, Japan
e-mail: mtakeda@kobe-u.ac.jp

Introduction

Circadian oscillation involves two interlocked transcriptional feed-back loops encompassing several circadian proteins, such as CLOCK (CLK), CYCLE (CYC), PERIOD (PER), TIMELESS (TIM), VRILLE (VRI), and PAR DOMAIN PROTEIN 1ε (PDP1ε) in *Drosophila melanogaster* (Allada et al. 1998; Blau and Young 1999; Cyran et al. 2003; Darlington et al. 1998; Rutila et al. 1998). One well-characterized transcriptional feed-back loop consists of the basic helix-loop-helix/*P*ER-*A*RNT-*S*IM (PAS) homology containing CYC and CLK, where CYC and CLK form a heterodimer that binds to E-box enhancer elements for *per* and *tim* transcription. The PER/TIM heterodimer interferes in some way with CLK-CYC binding to E-boxes (Hardin 2004). In another feed back loop, VRI and PDP1ε proteins bind VRI/PDP1ε-boxes to control *clk* transcription (Cyran et al. 2003; Glossop et al. 2003). A dominant negative form of CLK lacking most of the activation domain (*ClkJrk*) not only abolishes behavioral rhythms (Allada et al. 1998), but also eliminates molecular rhythms in fly heads (Ceriani et al. 2002; Claridge-Chang et al. 2001; McDonald and Rosbash 2001; Ueda et al. 2002).

Circadian rhythms in behavior are controlled by clock neurons. In *D. melanogaster*, a key set of clock-containing neurons located in the ventrolateral region of the accessory medulla is critical for robust locomotor rhythms (Ewer et al. 1992; Hardin et al. 1992; Frisch et al. 1994; Helfrich-Förster 1998; Renn et al. 1999). Recently, the distribution pattern of PER-like immunohistochemical reactivity (PER-ir) in several model insects has suggested that the master clock driving rhythmic behavior is located in the optic lobe (OL), in the dorsolateral protocerebrum, or in some other brain regions, e.g., the subesophageal ganglion (SOG) and the pars intercerebralis (PI; Závodská et al. 2003a, b; Sehadová et al. 2004; Shao et al. 2006).

In *D. melanogaster*, PER-, TIM-, CLK-, and CYC-immunoreactive neurons are located in the lateral protocerebrum (the lateral neuron) at the border to the OL and in the dorsal protocerebrum (the dorsal neurons; Helfrich-Förster 2004). The subcellular localization of PER, as predicted from the negative feed-back loop, is entirely nuclear at certain circadian times and cytoplasmic at other times. PER-ir occurs in the nucleus in a few other species, such as *Manduca sexta* in the dorsal protocerebrum (Wise et al. 2002), in the OL of *Pachymorpha maderae* (Frisch et al. 1996), and in the OL of *Leucophaea maderae* (Schneider and Stengl 2005), whereas in a great majority of insects, PER is detectable only in the cytoplasm. For example, only fluctuations in the cytoplasmic PER content without translocation into the nucleus have been found in the putative clock neurons of the moths, *Antheraea pernyi* (Sauman and Reppert 1996) and *Bombyx mori* (Sehadová et al. 2004), and no oscillations have been detected in *Manduca sexta* (Wise et al. 2002). This indicates that the functional mechanisms and neuronal networks of the clock differ among insects, despite the high structural conservation of clock proteins (for a review, see Helfrich-Förster 2005).

Hemimetabolous insects, such as cockroaches and crickets, have served as good experimental animals because of their relatively large nervous system with identifiable neurons that allow the search for neuronal components of the circadian system in the central nervous system (for a review, see Tomioka and Abdelsalam 2004). For locomotor rhythms, the OL has been recognized as the locus of the circadian pacemaker in cockroaches (Nishiitsutsuji-Uwo and Pittendrigh 1968) and crickets (Sokolove 1975; Tomioka and Chiba 1984; Abe et al. 1997), mostly based on surgical experiments that remove, transect, or extirpate the brain structure. Surgery at critical connectives causes arrhythmicity in the locomotor activity. Our previous results have demonstrated that PER-ir and casein kinase I α (CKIα)-ir are co-localized only in the proximal frontoventral (Pfv) of the OL in *Dianemobius nigrofasciatus* (Orthoptera: Gryllidae), but that in *Allonemobius allardi*, co-localization is observed only in the maxillary and

mandibular neuromere in the midline of the SOG (Shao et al. 2006). This suggests that the locus of circadian neurons may reside in different regions in the two closely related crickets, although our recent data have shown that immunoreactivity against some neuropeptides, such as crustacean cardioactive peptide (CCAP), corazonin, and diapause hormone (DH) are located in the maxillary and mandibular neuromere of the SOG in both species (Sehadová et al. 2007). Following an investigation into core oscillator elements (Shao et al. 2006) and output elements (Sehadová et al. 2007), we have examined the detailed localization and temporal expression patterns of the transcription modulators in *A. allardi* sampled at 4-h intervals throughout a 24-h period and under different photoperiodic conditions. Double-labeling has also been applied to investigate the co-localization of these antigens. CYC and CLK play important roles in circadian clock regulation in *D. melanogaster* and may also be involved in the transcriptional regulation of other functions.

Materials and methods

Animals

Crickets, *A. allardi* (Orthoptera: Gryllidae: Nemobiinae), were collected from South Carolina (34° N, 82° W; see Shao et al. 2006). They were kept under a light:dark regime (LD) of 16:8 (16 h light and 8 h darkness) or LD 12:12 at 25°C and fed with commercial artificial diets (MF mix, Oriental Yeast, Tokyo, Japan). LD 12:12 accelerated larval development and induced egg diapause in the progeny (Q.-M. Shao, unpublished). Dim red light was used for dissection during the dark phase (a 60-W bulb shielded with a 660-670 nm cut-off Kodak 1A filter was placed 1 m above the insect).

Primary antibodies

To obtain recombinant CYC and CLK protein, cDNAs corresponding to the 496th to 686th amino acids (191 amino acids, containing PAS B partially and near the C-terminal) of *B. mori* CYCb (*Bm*CYCb; 700 amino acids) and to the 378th to 562nd amino acids (185 amino acids, containing a region near the C-terminal) of CLK (584 amino acids) cloned from the pupal brain of *B. mori* (*Bm-cycb*; Markova et al. 2003; GenBank accession no. AB073712.1; *Bm-clk*; Markova et al., unpublished) were subcloned into pET22b in-frame and upstream of 6xHis. Recombinant *Bm*-CYCb and *Bm*-CLK proteins induced in BL21 (DE3) *Escherichia coli* as *Bm*-CYCb-6xHis, and *Bm*-CLK-6xHis fusion proteins. The amino acid alignments of *B. mori* CYC and CLK and of *A. pernyi*

CYC and CLK are shown in Figs. 1, 2, respectively. The amino acids underlined were designed for making the recombinant proteins for producing the antibodies and show high homology between the respective insects.

All recombinant proteins in Freund's complete adjuvant were injected under the skin of male New Zealand White rabbits and male Wistar rats at multiple sites. One week intervals, booster immunizations were carried out several times together with monitoring the antibody titer by enzyme-linked immunosorbent assay (ELISA), Western blotting, and immunohistochemistry. After confirmation of a high titer, blood was drawn under deep anesthesia. We confirmed by ELISA that the anti-*Bm*-CYC rat serum and anti-*Bm*-CLK rat serum did not recognize *Bm*-CLK-6xHis

and *Bm*-CYCb-6xHis, respectively. These assays indicated that the IgG contained in these sera did not recognize the fusion tag moiety but *Bm*-CYC, or *Bm*-CLK moiety.

Pre-absorption was conducted for the rabbit CYC antibody to test for antibody specificity. The CYC antigen (175 ng/ml) was added to the anti-CYC antibody (1:1,000) in a normal serum solution for preabsorption and incubated overnight at 4°C. Immunohistochemistry was conducted the next day. When the primary antibody solution was replaced with the preabsorbed antibody solution, CYC-ir vanished. This CYC antibody stained the same cells as those stained by dCYC antibody, a generous gift from Dr. I. Edery. The CYC antibody raised in rat was used in double-labeling experiments, and its specificity was established in
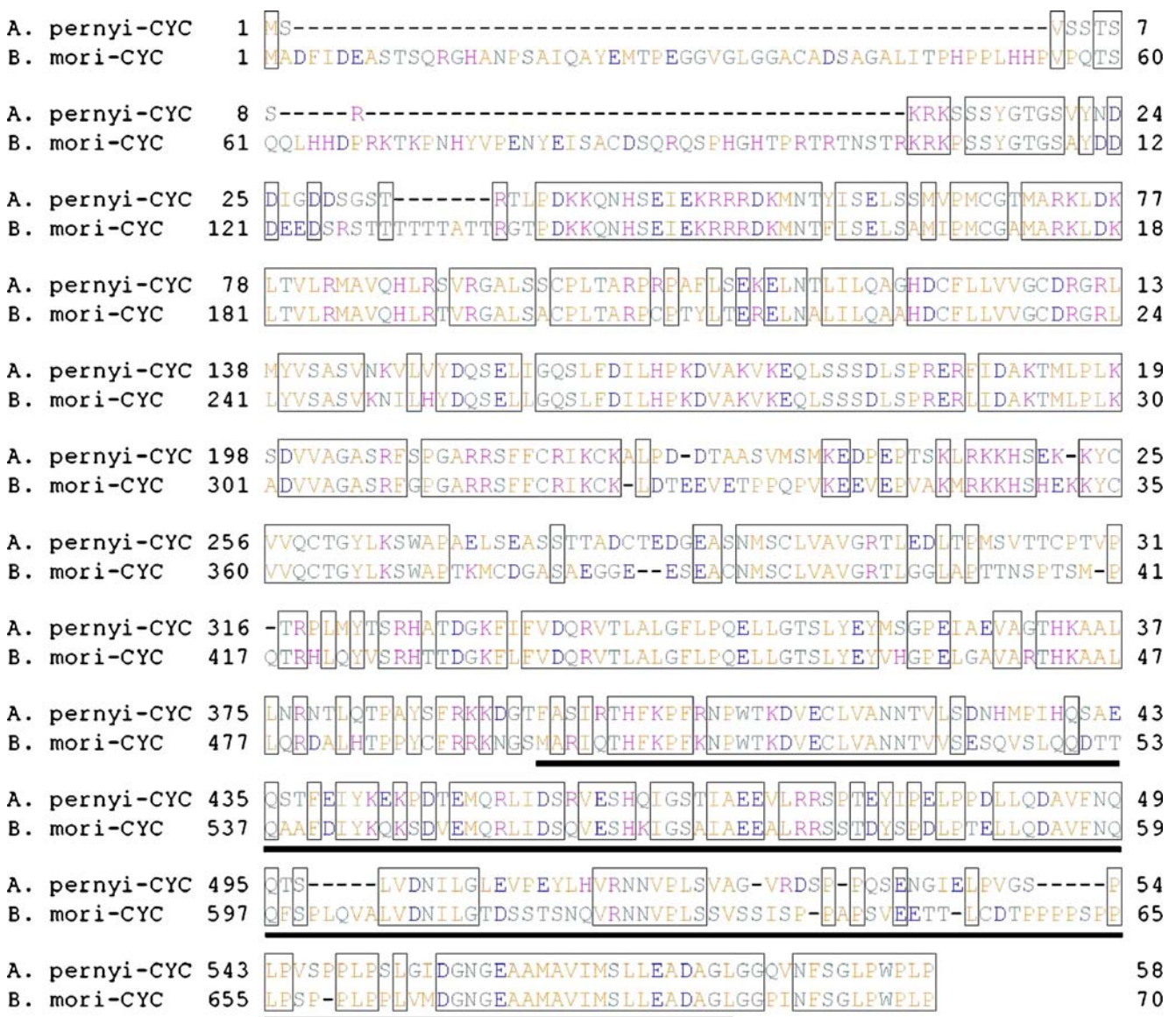

Fig. 1 Amino acid alignment of *Bm*CYC (BAB91178) and *Ap*CYC (AAR14937). The *underlined* portion was used as antigen to raise antibody against *Bm*CYC

the same way as for the rabbit CYC antibody. The rabbit CLK antibody showed unique reactivity in most regions, when compared with the CYC antibody, but showed co-localization in the midline group neurons of the SOG, and hence, possibly with CCAP-ir, and DH-ir (Sehadová et al. 2007).

Immunohistochemistry

Whole heads were separated from anesthetized animals in sterile saline and fixed overnight at 4°C in Bouin's solution (15 vol picric acid, 5 vol formalin, 1 vol acetic acid). The insects were dissected during the dark phase under dim light at 660-670 nm wavelengths. Standard techniques were employed to prepare tissue sections (8 μm) in paraffin. Following deparaffination, sections were washed in TRIS-buffered saline (TBS; 0.05 M TRIS-HCl, pH 7.6) and

blocked with 1.5% normal goat serum diluted in TBS for 1 h at room temperature. They were then incubated with the respective primary antibody overnight at 4°C. Bound IgG was detected with the rabbit IgG-Vectastain Elite ABC kit (Vector Laboratories, Burlingame, Calif.) following the procedures described in Shao et al. (2006). The activity of the horseradish peroxidase (HRP) in the ABC was visualized with hydrogen peroxide (0.005%) and 3,3′-diaminobenzidine tetrahydrochloride (DAB, 0.25 mM in 0.1 M TRIS-HCl, pH 7.5). Stained sections were mounted in Biolet medium (Kouken Rika, Osaka, Japan) and visualized under a BX50F4 microscope (Olympus, Japan).

Double-labeling was conducted with sections that were consecutively treated with two combinations of primary and secondary antibodies. The rat anti-CYC antibody was followed by the biotinylated goat anti-rat IgG antibody. The rabbit antibody against CLK was first visualized by
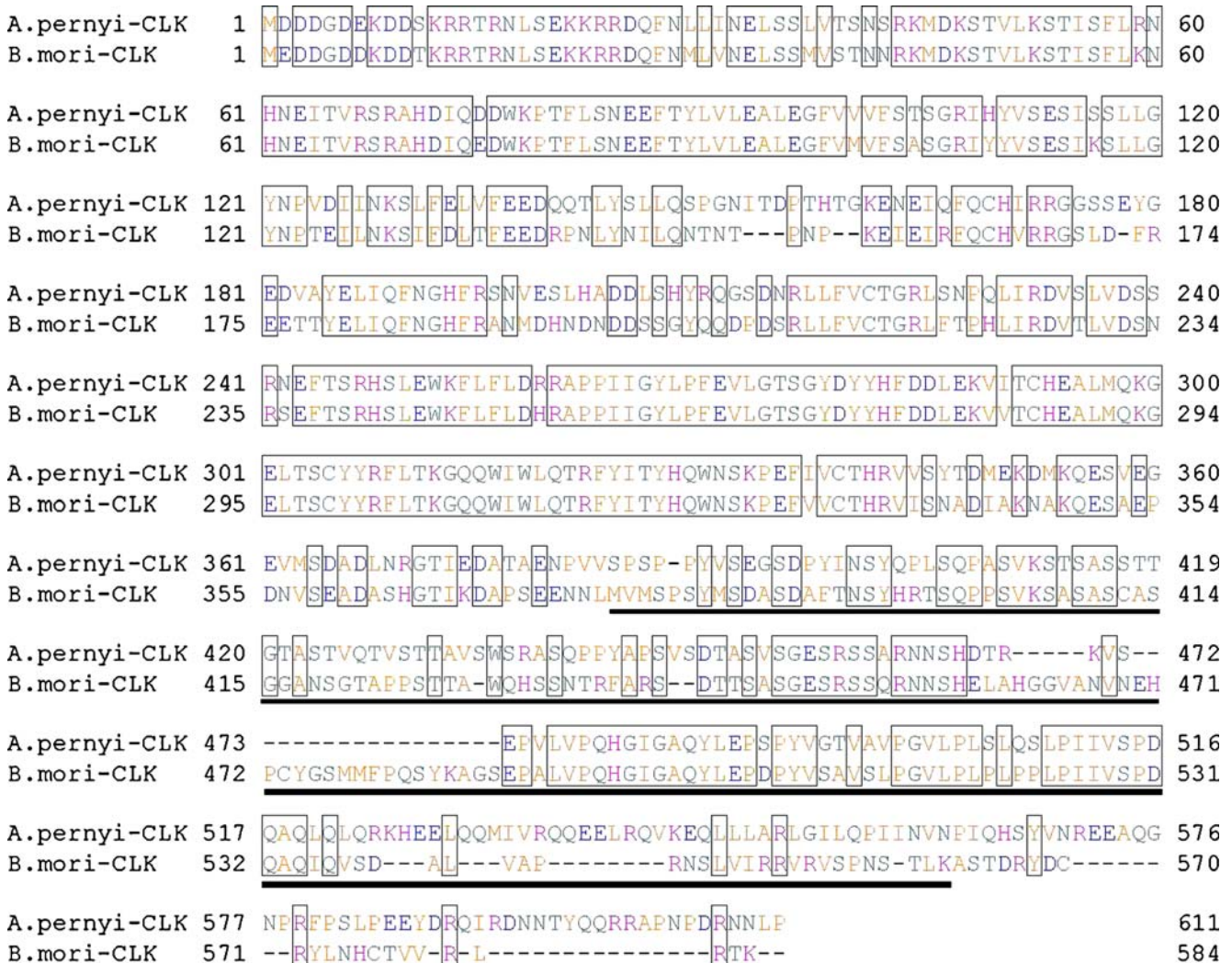


```
A.pernyi-CLK   1  MDDDGDEKDDSKRRTRNLSEKKRRDQFNLLINELSSLVTSNSRKMDKSTVLKSTISFLRN   60
B.mori-CLK     1  MEDDGDDKDDTKRRTRNLSEKKRRDQFNMLVNELSSMVSTNNRKMDKSTVLKSTISFLKN   60

A.pernyi-CLK  61  HNEITVRSRAHDIQDDWKPTFLSNEEFTYLVLEALEGFVVFSTSGRIHYVSESISSLLG  120
B.mori-CLK    61  HNEITVRSRAHDIQEDWKPTFLSNEEFTYLVLEALEGFVMVFSASGRIYYVSESIKSLLG  120

A.pernyi-CLK 121  YNPVDIINKSLFELVFEEDQQTLYSLLQSPGNITDPTHTGKENEIQFQCHIRRGGSSEYG  180
B.mori-CLK   121  YNPTEILNKSIEDLTFEEDRPNLYNILQNTNT---PNP--KEIEIRFQCHVRRGSLD-FR  174

A.pernyi-CLK 181  EDVAYELIQFNGHFRSNVESLHADDLSHYRQGSDNRLLFVCTGRLSNPQLIRDVSLVDSS  240
B.mori-CLK   175  EETTYELIQFNGHFRANMDHNDNDDSSGYQQDPDSRLLFVCTGRLFTPHLIRDVTLVDSN  234

A.pernyi-CLK 241  RNEFTSRHSLEWKFLFLDRRAPPIIGYLPFEVLGTSGYDYYHFDDLEKVITCHEALMQKG  300
B.mori-CLK   235  RSEFTSRHSLEWKFLFLDHRAPPIIGYLPFEVLGTSGYDYYHFDDLEKVVTCHEALMQKG  294

A.pernyi-CLK 301  ELTSCYYRFLTKGQQWIWLQTRFYITYHQWNSKPEFIVCTHRVVSYTDMEKDMKQESVEG  360
B.mori-CLK   295  ELTSCYYRFLTKGQQWIWLQTRFYITYHQWNSKPEFVVCTHRVISNADIAKNAKQESAEP  354

A.pernyi-CLK 361  EVMSDADLNRGTIEDATAENPVVSPSP-PYVSEGSDPYINSYQPLSQPASVKSTSASSTT  419
B.mori-CLK   355  DNVSPADASHGTIKDAPSEENNLMVMSPSYMSDASDAFTNSYHRTSQPPSVKSASASCAS  414

A.pernyi-CLK 420  GTASTVQTVSTTAVSWSRASQPPYAPSVSDTASVSGESRSSARNNSHDTR-----KVS--  472
B.mori-CLK   415  GGANSGTAPPSTTA-WQHSSNTRFARS--DTTSASGESRSSQRNNSHELAHGGVANVNEH  471

A.pernyi-CLK 473  ----------------EPVLVPQHGIGAQYLEPSPYVGTVAVPGVLPLSLQSLPIIVSPD  516
B.mori-CLK   472  PCYGSMMFPQSYKAGSEPALVPQHGIGAQYLEPDPYVSAMSLPGVLPLPLPPLPIIVSPD  531

A.pernyi-CLK 517  QAQLQLQRKHEELQQMIVRQQEELRQVKEQLLLARLGILQPIINVNPIQHSYVNREEAQG  576
B.mori-CLK   532  QAQIQVSD---AL---VAP--------RNSLVIRRVRVSPNS-TLKASTDRYDC------  570

A.pernyi-CLK 577  NPRFPSLPEEYDRQIRDNNTYQQRRAPNPDRNNLP                          611
B.mori-CLK   571  --RYLNHCTVV-R-L---------------RTK--                          584
```

Fig. 2 Amino acid alignment of *Bm*CLK (E.P Markova, unpublished) and *Ap*CLK (AAR14936). The *underlined* portion was used as antigen to raise antibody against *Bm*CLK

hydrogen peroxide and DAB (as above), and then the second visualization was conducted with hydrogen peroxide (0.005%) and Chromogen (Vector Laboratories, SK-4700, Burlingame, U.S.A.) (purple; 150 µl in 5 ml 0.1 M phosphate-buffered saline, pH 7.4).

Assessment of immunostaining intensity

The intensity of staining was assessed on DAB-stained preparations processed under identical conditions. The length of exposure to DAB was set in preliminary runs to 10 min for both the CYC and the CLK antibody. Three generations of crickets were examined independently at Zeitgeber time 0 (ZT0), ZT4, ZT8, ZT12, ZT16, and ZT20. Each of these six groups included several males and females. All the preparations of a time series were processed simultaneously. The intensity of staining was scored by two independent observers with an arbitrary scale ranging from 0 (no reaction) to 4 (maximal response). Each preparation was first evaluated independently and was then compared with others of the same time series and finally with the preparation of the corresponding circadian time in another

insect generation. Values in the Results represent the intensities found in most of the preparations examined for each antibody at each time point (Shao et al. 2006).

Results

CYC-like immunoreactivity

CYC-ir was observed in the protocerebrum, tritocerebrum, deutocerebrum, frontal ganglion (FG) and SOG, but the accessory medulla region of the OL showed no staining (Table 1, Fig. 3a). Males and females showed no differences in staining. CYC-ir was mostly cytoplasmic. A strongly stained structure was located in the compound eyes and resembled the Hofbauer-Buchner (H-B) eyelet in *D. melanogaster*, although ontogenic or functional correspondence has not been confirmed (Fig. 3b, arrow). Three small weakly stained neurons with axonal projection to the lamina region were located in the proximal frontodorsal (Pfd) region of the OL (Fig. 3c, arrow). One neuron with a long slim neuronal process extending to the corpus

Table 1 Numbers (mean or mean±SD) and staining intensity of CYC- and CLK-immunopositive cells in the cephalic ganglia of the ground cricket, *A. allardi*

Ganglion region		Cell numbers, staining intensity*	
		CYC (*n*=6)	CLK (*n*=6)
OL	Pfv cluster, large cells	-	-
	Pfv cluster, small cells	-	5.83±0.69, +++
	Pfd, small cells	3, +++	-
Pr	Base of the optic stalk	2++	2, ++
	Posterolateral cortex	2, +++	1, ++
	PI, dorsal#	17.6±1.59 ++++	12±1.29, +++
	PI, ventral#	4, ++	10.2±1.72, ++
	DL, large cells	1, ++	2, ++++
	DL, small cells	3, +++	5, ++++
De	Cortex region	2, +++	-
Tr	Medial region	4.66±0.47, ++++	4.66±0.47, ++++
SOG	Mdb-Vm#	5.16±0.69, +++	5.16±0.69, +++
	Mxl-Vm#	9.5±0.96, +++	9.66±0.47, +++
	Mxl-L	1, ++++	1, ++++
	Lb-Vm#	2, ++	10±1.67, ++
FG	Cells#	4, ++++	-
	Arborization	++	++++
CC	Cortex arborization	++	++
	Central arborization	-	-
NCA I		++++	++++

*Immunoreactivity was quantified as absent (-), weak (+), moderate (++), considerable (+++), and strong (++++). Evaluation scales were set for each antibody separately. Cell numbers are shown either for the entire ganglion (#) or for half of it, e.g., one brain hemisphere or one optic lobe (*CYC* Cycle, *CLK* Clock, *Pfv* proximal frontoventral, *Pfd* proximal frontodorsal, *Pr* protocerebrum, *PI* pars intercerebralis, *De* deutocerebrum, *DL* dorsolateral region of the protocerebrum, *Tr* tritocerebrum, *SOG* subesophageal ganglion, *Mdb-Vm*, *Mxl-Vm*, *Lb-Vm* ventromedial cell clusters in the mandibular, maxillary, and labial neuromere, respectively, *Mxl-L*, *Lb-L* lateral cells in the maxillary and labial neuromere, respectively, *FG* frontal ganglion, *CC* corpora cardiaca, *NCAI* nervi corporis allati I)
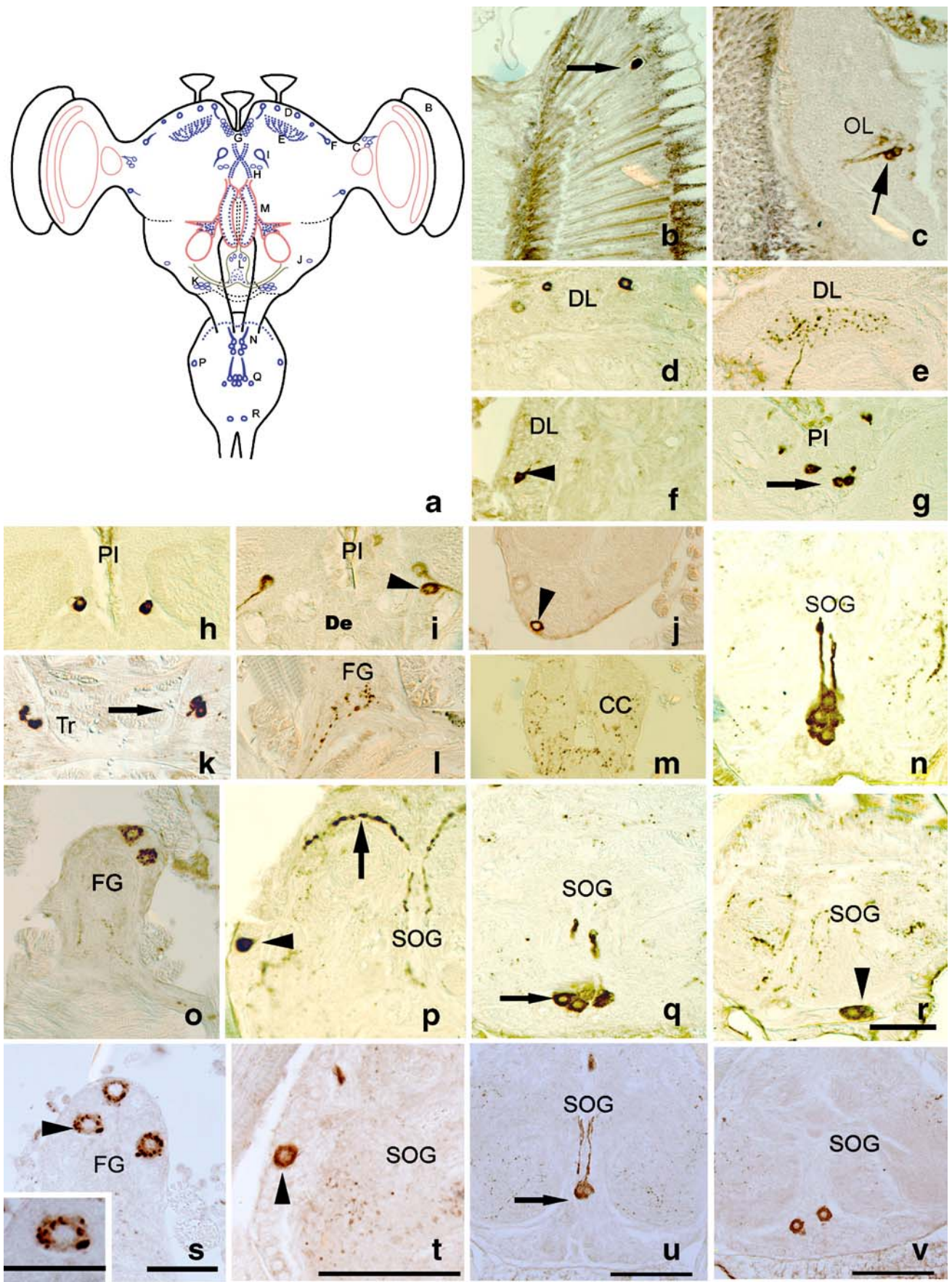
◄ **Fig. 3** CYC-ir in the brain-SOG complex of *A. allardi*. **a** Representation of the numbers and topography of CYC-immunoreactive cells in the brain-SOG and possible pathways of their nerve process (*letters* corresponding regions in **b–v**). **b** A strongly stained structure (*arrow*) located in the compound eye (resembles H-B eyelet in *D. melanogaster*). **c** Neurons located in Pfd region of the optic lobe (*OL, arrow*). **d** One large and one small cell situated in the dorsolateral (*DL*) region. **e** Neuronal arborization stained in the mushroom body calyx of the protocerebrum. **f** One neuron with short axonal process located in the DL region and sitting close to the OL (*arrowhead*). **g** Strongly stained cell bodies in the dorsal pars intercerebralis (*PI, arrow*). **h** Neurons located in the posteriolateral cortex of the protocerebrum. **i** Two neurons in the posterior PI with long neuronal processes (*arrowhead*) probably projecting to the ipsilateral corpus cardiacum (CC). **j** One moderately stained cell body in the deutocerebrum (*arrowhead*). **k** Representative cells located in the tritocerebrum (*Tr, arrow*). **l** Neuron arborization in the center region of the frontal ganglion (*FG*). **m** CYC-ir in the cortex of the *CC*. **o** Two representative large neurons in the anterior region of the FG. **n, p–r** CYC-ir in the SOG. **n** A group of neurons in the mandibular neuromere region. **p** One neuron in the lateral maxillary neuromere region of the SOG (*arrowhead*); the intensely immunostained neuronal process starting from the medial region of the SOG projects upward to the anterior region, then turns back along the lateral part of the SOG, and disappears (*arrow*). **q** Neurons in the maxillary neuromere region (*arrow*). **r** One of the cells in the labial neuromere region (*arrowhead*). **s** Three large cell bodies located in the FG in the fifth instar stage; one of the cell bodies is shown at higher magnification in the *inset*. **t** One large cell (*arrowhead*) situated in the lateral region of the SOG in the fifth instar. **u** Representative neuron (*arrow*) in the mandibular neuromere of the SOG in the fifth instar. **v** Two neurons located in the maxillary neuromere of the SOG in the fifth instar. *Bars* 100 μm

cardiacum (CC) and/or corpus allatum (CA) and another cell body with no visible axonal process were observed in the optic tract region (data not shown). One large and three small strongly stained neurons were situated in the dorsolateral (DL) region of the protocerebrum (Fig. 3d). Arborization of neuronal projections in the calyx of the peduncles was observed, but the staining could not be traced to the cell body (Fig. 3e). One large neuron with neurites projecting to the medial protocerebral region was observed near the optic tract region (Fig. 3f, arrowhead). Approximately nine strongly stained cell bodies were located at each hemisphere of the dorsal PI (Fig. 3g, arrow), with two lying more ventrally. Four large-sized neurons per brain were present, two of which had long axonal neurites probably projecting to the ipsilateral CC (Fig. 3i), and two cell bodies were located in the posteriolateral cortex of the protocerebrum (Fig. 3h). One cell body was moderately stained in each of the deutocerebrum regions (Fig. 3j, arrowhead), and a group of approximately five cell bodies was strongly stained in each tritocerebrum (Fig. 3k, arrow). The FG harbored intense CYC-ir, with four large strongly stained cell bodies in the anterior cortex region (Fig. 3o) and abundant neuronal arborization in the posterior region (Fig. 3l). CYC-ir was observed in the cortex of the CC (Fig. 3m) and in the nervi corporis allati I (NCAI), whereas no obvious staining was found in the CA.

The SOG harbored four groups of neurons: 4-6 in the mandibular neuromere region (Fig. 3n) and ten in the maxillary neuromere region (Fig. 3q, arrow). Intensely stained neurites extending from these two clusters of neurons formed two parallel bundles running along the dorsal SOG midline to the circumesophageal connectives (Fig. 3n). One strongly stained cell body was found in each lateral maxillary neuromere region (Fig. 3p, arrowhead), and two cell bodies in the labial neuromere region were also strongly stained (Fig. 3r, arrowhead). A strongly stained axonal process was traced from the labial neuromere to the dorsal region and then turned backward laterally to the ventral region (Fig. 3p, arrow). The expression of CYC-ir in the fifth instar nymph of *A. allardi* was almost the same as that in the adult stage. The CYC-ir was granular in the cytoplasm in the FG (Fig. 3s). In the SOG, one large neuron was observed in the lateral maxillary neuromere region (Fig. 3t, arrowhead), a cluster of 4-6 neurons as found in the mandibular neuromere (Fig. 3u, arrow), and eight to ten neurons were stained in the maxillary neuromere (Fig. 3v).

The temporal pattern in the CYC-ir was examined with individuals being dissected at 4-h intervals throughout a 24-h period under two photoperiods (LD 12:12 and LD 16:8). However, no daily fluctuations were detected for these photoperiods with regard to the number of cells and the distribution and intensity of immunoreactivity.

CLK-like immunoreactivity

Basically, CLK-ir resembled CYC-ir (Table 1) but was expressed more widely in the cephalic ganglia of *A. allardi*, including the OL and central body. No CLK-ir was observed in the deutocerebrum (Fig. 4a). About six small cells, each with strongly stained somata were situated in the Pfv region of the OL (Fig. 4b, arrow). Two large strongly stained cell bodies and five small cell bodies per hemisphere were located in the DL region of the protocerebrum, with one large neuron having a long neuronal projection toward the mushroom body calyx (Fig. 4d). Another group of three small cells was located in the dorsolateral protocerebrum close to the OL (Fig. 4c, arrow). A similar CYC-ir arborization was found in the mushroom body calyx, but tracing was possible only to the ventrolateral protocerebrum (data not show). One neuron probably sent a thin process to the CC and/or the CA, and another cell body with no such process was observed in the optic stalk (Fig. 4f, arrowhead). In total, approximately 12 cells were located in the dorsal PI, approximately ten in the ventral PI (Fig. 4i, arrow), and one was seen in the posteriolateral cortex of the protocerebrum. A group of approximately five cell bodies was located in the center of the tritocerebrum (Fig. 4e, arrow). The FG harbored no CLK-ir neurons but
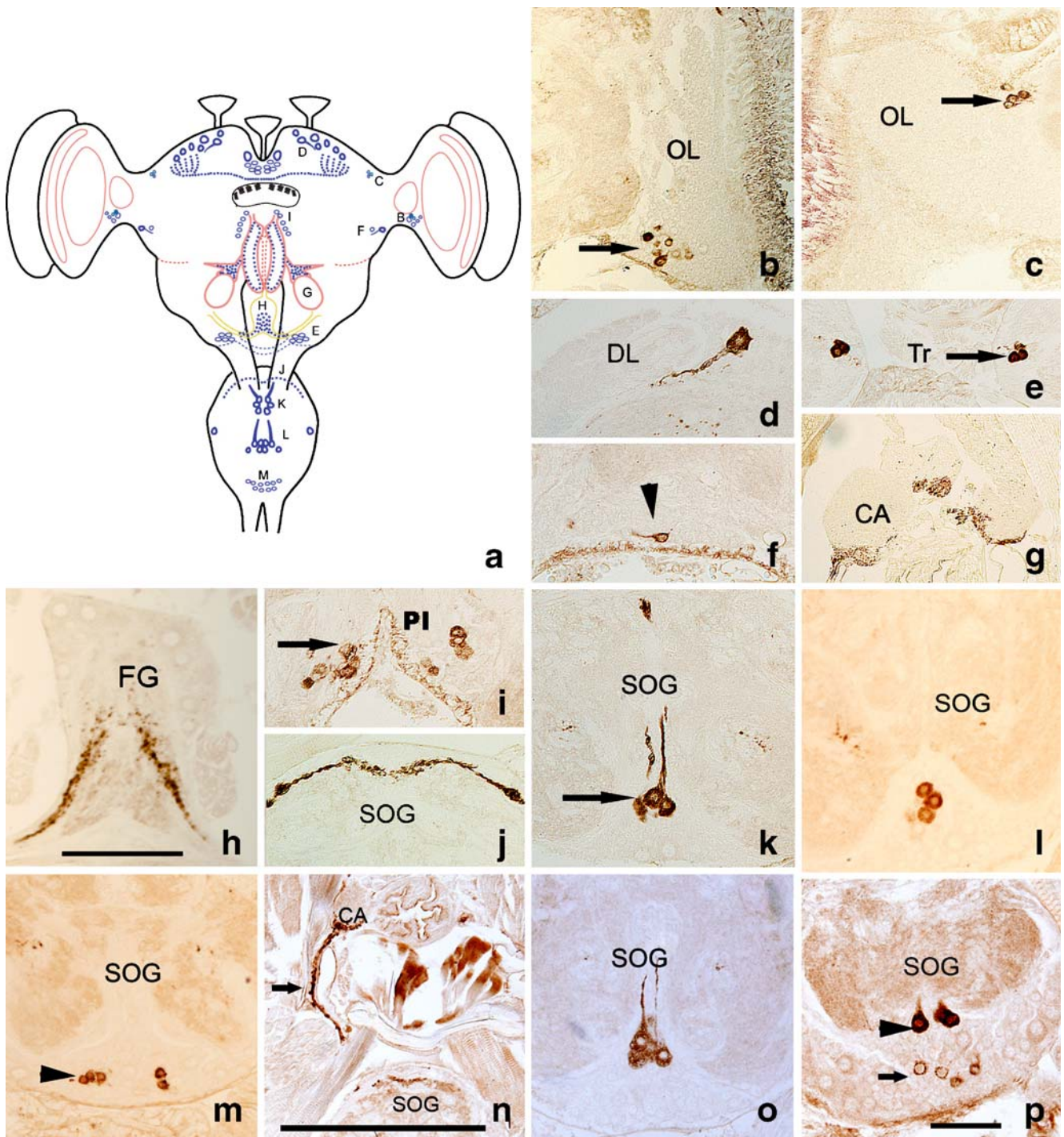
exhibited intense neuronal arborization in the posterior-medial region (Fig. 4h). As for CYC-ir, CLK-ir was observed in the cortex of the CC and NCAI, but the CA was free of staining (Fig. 4g). In the SOG, strongly stained neuronal fibers extended from the mandibular region frontally and turned laterally, as for CYC-ir, although double-labeling could not verify their identity (Fig. 4j). CLK-ir occurred in the mandibular neuromere and in the maxillary and labial neuromeres on the SOG midline

(Fig. 4k, l). Strong CLK-ir was found in fibers leaving the mandibular neuromere midline cells frontally (Fig. 4k, arrow). Approximately ten small strongly stained CLK-ir neurons were located in the labial neuromere region of the SOG (Fig. 4m, arrowhead). CLK-ir in the fifth instar nymph was also studied; the distribution of CLK-ir was found to be identical with that at the adult stage. A clear neuronal process was traced from the CA to the SOG in the nymphal stage (Fig. 4n, arrow). Eight to ten large neurons

◄ **Fig. 4** CLK-ir in the brain-SOG complex of *A. allardi*. **a** Represen-
tation of the numbers and topography of CLK-immunoreactive cells
in the brain-SOG and possible pathways of their nerve processes
(*letters* corresponding regions in **b–p**). **b** Group of cells (*arrow*)
located in the Pfv region of the *OL*. **c** Representative cells (*arrow*) in
the DL region close to the OL. **d** A large strongly stained neuron with
long axonal process in the *DL* region. **e** Representative cells in the
tritocerebrum (*Tr*, *arrow*). **f** Neuron with a slim axonal process
(*arrowhead*) at the base of the optic stalk. **g** Neuronal arborization in
the cortex of the CC and NCAI (*CA corpus allatum*). **h** Extensive
neuronal arborization in the FG. **i** Representative cell bodies in the
posterior *PI* (*arrow*). **j** An intensely immunostained neuronal process
starting from the medial region of the *SOG*, projecting upward to the
anterior region, and then turning back along the lateral part of the
SOG, where it disappears. **k** Large neurons with intensely immuno-
stained axonal process located in the mandibular neuromere of the
SOG (*arrow*). **l** A group of cell bodies in the maxillary neuromere of
the SOG. **m** Representative cell bodies (*arrowhead*) situated in the
labial neuromere region of the SOG. **n** A strongly immunostained
neuronal process started from the CA was found to extend to the SOG
in the fifth instar (*arrow*). **o** A cluster of large neurons with a strongly
immunostained axonal process located in the mandibular neuromere
region of the SOG in the fifth instar. **p** Large neurons (*arrowhead*)
situated in the maxillary neuromere region of the SOG in the fifth
instar. Several small and weak stained neurons (*arrow*) were located in
the labial neuromere region of the SOG. *Bars* 100 μm

formed a cluster in the mandibular neuromere of the SOG
(Fig. 4o). Four to six large neurons were situated in the
maxillary neuromere of the SOG (Fig. 4p, arrowhead), with
several weakly stained cell bodies in the labial neuromere
(Fig. 4p, arrow).

The temporal expression pattern was analyzed for CLK-
ir in individuals dissected at 4-h intervals throughout a
24-h period under LD 12:12 and 16:8. However, no
obvious daily fluctuations were detected for these photo-
periods with regard to the number of cells and the
distribution and intensity of immunoreactivity.

Co-localization of CYC-ir and CLK-ir

As Table 1 shows, CYC-ir and CLK-ir occurred in the same
regions. For a detailed investigation of possible co-
localization patterns, double-labeling was conducted. The
results showed that CYC- and CLK-ir cells and processes
were not always identical. For example, CYC-ir and CLK-
ir were both expressed in the PI region but were not co-
localized (Fig. 5a), and CYC- and CLK-immunoreactive
neurons and processes were not identical in the OL. The
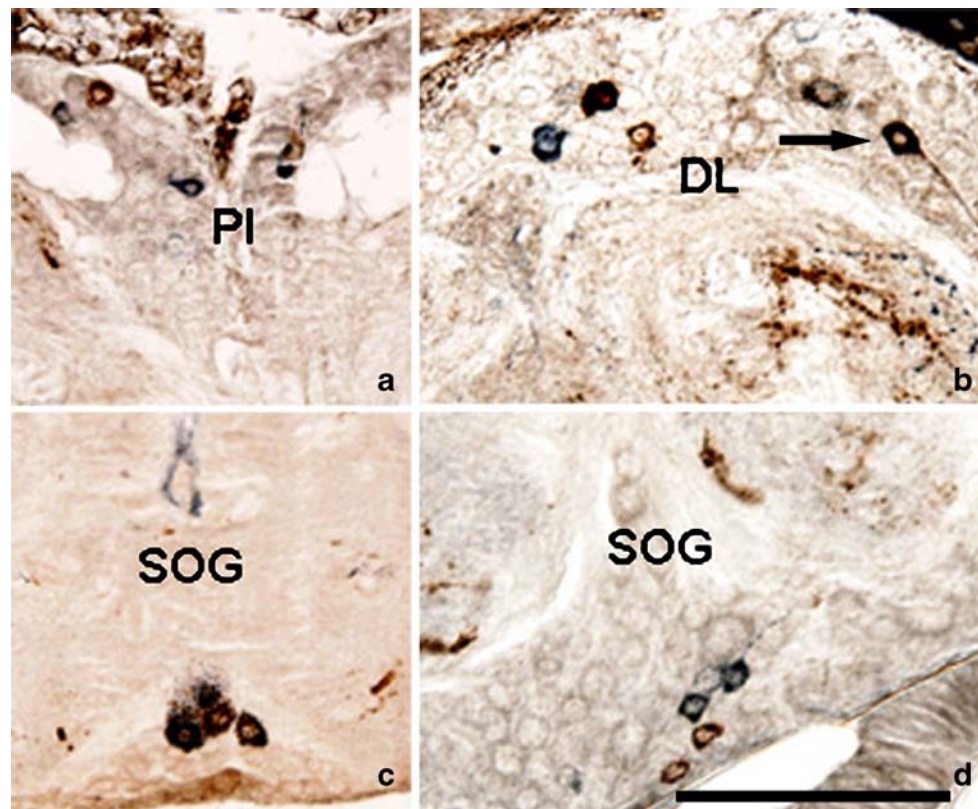cell bodies and neuronal processes in the DL region were

Fig. 5 Co-localization of CYC-ir and CLK-ir in *A. allardi*. CLK-ir
(*brown*) and CYC-ir (*purple*) in the pars intercerebralis (*PI*, **a**) and in
the dorsolateral region (*DL*) of the protocerebrum (**b**), and one of the
neurons probably co-labeling with both CYC-ir and CLK-ir (**b**,
arrow). CYC-ir (*brown*) and CLK-ir (*purple*) were co-expressed in
the mandibular region of the *SOG* (**c**). CYC-ir (*brown*) or CLK-ir
(*purple*) in the labial neuromere of the *SOG* (**d**). *Bar* 100 μm

partially co-labeled with both the antibodies. One of the neurons stained was probably double-stained with both antibodies (Fig. 5b, arrow), whereas most of the other CYC-ir and CLK-ir were unique (Fig. 5b). The neuronal processes from the ventral PI, extending to the tritocerebrum region, were specific for CYC-ir, and the neurons located in the ventral PI region were specific for CLK-ir (data not show). The cell bodies situated in the center of the tritocerebrum were double-stained (data not show). The cell bodies stained in the mandibular and maxillary regions in the midline of the SOG exhibited CYC-ir and CLK-ir (Fig. 5c). However, CYC-ir and CLK-ir in the labial neuromere were not co-localized (Fig. 5d), the neuronal processes spread in the SOG being unique for either CYC or CLK.

Discussion

We have previously investigated the distribution of three clock proteins, i.e., PER, CKIε, and cryptochrome (CRY; Shao et al. 2006) and three neuropeptides, i.e., CCAP, corazonin, and DH (Sehadová et al. 2007) in the cephalic ganglia of the adult ground cricket, *A. allardi* by immunohistochemistry. We have found that most of the circadian-related proteins or peptides that we have investigated are prominently expressed in the mandibular and maxillary clusters of neurons in the midline of the SOG and also in the clustered cell bodies of the tritocerebrum. Furthermore, all of the clock-related proteins that we have investigated have been observed mainly in the cytoplasm and show no daily oscillation in the number and staining intensity of neurons with the samples being prepared at 4-h intervals throughout a 24-h period.

The heterodimerization of the CYC and CLK proteins is critical for them to serve as a transcriptional regulator in *Drosophila* in which the CLK protein or at least the amount of CLK protein has been suggested to be the component limiting the levels of CLK-CYC complexes in the nucleus (Bae et al. 2000). Immunohistochemistry and in vitro DNA-binding experiments have shown that CLK is present at constant levels in the nucleus throughout a 24-h period (Wang et al. 2001; Houl et al. 2006); this contrasts with the cycling shown by Western blotting (Lee et al. 1998; Bae et al. 2000). CLK protein is present in all the canonical brain oscillator cells including three groups in the lateral protocerebrum and three groups of neurons in the dorsal brain in *D. melanogaster* (Houl et al. 2006). In *Drosophila*, *cyc* mRNA expression is constant (Rutila et al. 1998). CYC-ir is constantly expressed in the cytoplasm of the neurons in the silkworm, *B. mori* (Sehadová et al. 2004), as is the *cyc* mRNA level detected by Northern blotting (Markova et al. 2003). CYC protein is present, in the

lateral protocerebrum, in four large neurons that also express PER protein in *B. mori* (Sehadová et al. 2004).

In this report, we have investigated CYC-ir and CLK-ir in *A. allardi*. Levels of CYC-ir and CLK-ir show no oscillation at 4-h intervals throughout a 24-h period. Both CYC-ir and CLK-ir are expressed in the cytoplasm prominently in cells of the protocerebrum, tritocerebrum, OL, SOG, FG, and CC. Although generally similar, some differences exist between the CYC-ir and CLK-ir patterns, such as in the OL in which CYC-ir occurs only in three cell bodies at the Pfd region, whereas CLK-ir is found in approximately six cell bodies in the Pfv region. CLK-ir may partially co-localize with PER-ir in the Pfv region, although double-labeling has not been conducted because of the short supply of the PER antibody (Shao et al. 2006). The deutocerebrum harbors a moderately stained CYC-immunoreactive neuron, whereas CLK-ir is absent in this region. A group of closely clustered CYC- and CLK-immunopositive cell bodies have been observed in the tritocerebrum, whereas PER-ir is found between the deuto-cerebrum and tritocerebrum (Shao et al. 2006). The close spatial relationship between CYC-ir, CLK-ir, and PER-ir probably indicate the functional importance of these regions. A striking difference has been noted in the FG, in which CYC-ir occurs in four large cell bodies, whereas CLK-ir neurons are absent, but intensely stained neuronal arborization has been observed. The intensely CLK-ir neuronal arborization in the FG is consistent with the PER-ir, CRY-ir, corazonin-ir, and DH-ir in this species. Large neurons with no detectable projections in the FG have also been observed with Doubletime (DBT)/CKIε-ir and CCAP-ir. These reactivities are probably co-localized with each other, although double-labeling has not been conducted because of a shortage of the antibody (Shao et al. 2006; Sehadová et al. 2007). CYC-ir and DBT-ir have been recognized in some large neurons in the FG of *B. mori* suggesting that the FG has important functions in the circadian rhythm (Sehadová et al. 2004). Of note, transcription factors have only been found in the cytoplasm, a result that is a mystery, but this pattern has also been detected in *B. mori* (Sehadová et al. 2004). Their presence in limited amounts in the nucleus still remains as a possibility.

In *Drosophila*, all dCLK-immunoreactive cells contained CYC. Moreover, at all C-terminals, essentially all the dCLK is stably bound to CYC (Bae et al. 2000). However, in our double-labeling experiments, CYC-ir and CLK-ir are only partially co-expressed in *A. allardi*, being co-localized in the mandibular and maxillary neuromeres of the midline in the SOG and in the tritocerebrum. One middle-sized neuron in the DL region shares CYC-ir and CLK-ir. However, depending on the position and size of the neurons in the DL region, we consider that some of the

large neurons may share CLK-ir and PER-ir, whereas such neurons have not been observed to contain CYC-ir. One neuronal process partially co-stains with CYC-ir and CLK-ir in the DL region of the protocerebrum, whereas other stained neurons and neuronal fibers are uniquely immunostained for these proteins. These results show that CYC and CLK are not always bound together in neuronal cell bodies or in their processes; thus, in other words, CYC or CLK may have a dimerization pattern other than with each other. Species-specific associations of clock proteins are known in other species, for example, in *Danaus plexippus* in which the suppressor of the regulator, i.e., CYC and CLK, is not PER but CRY (Zhu et al. 2005). Alternatively, the relative quantities of CYC and CLK may differ at different clock neurons. Nevertheless, they may co-operate with each other in special neurons but make a variety of functional association at each locus. The SOG may serve as the most important element in the circadian system of this species, because the immunoreactivities of many circadian-related proteins including PER, DBT/CKIα, CRY, CYC, and CLK, are located in this region. This seems contradictory to the idea that OL serves as the central pacemaker in at least *Pteronemobius nigrofasciatus*, depending on the surgical and immunohistochemical experiments performed (Shimizu and Masaki 1997; Shao et al. 2006). Surgical experiments will be important to provide stronger evidence for SOG being the most important circadian elements in the ground cricket, *A. allardi*.

References

Abe Y, Ushirogawa H, Tomioka K (1997) Circadian locomotor rhythm of the cricket, *Gyllodes sigillatus*. I. Localization of the pacemaker and the photoreceptor. Zool Sci 14:719–727

Allada R, White NE, So WV, Hall JC, Rosbash M (1998) A mutant *Drosophila* homology of mammalian *clock* disrupts circadian rhythms and transcription of *period* and *timeless*. Cell 93:791–804

Bae K, Lee C, Hardin PE, Edery I (2000) dCLOCK is present in limiting amounts and likely mediates daily interactions between the dCLOCK-CYC transcription factor and the PER-TIM complex. J Neurosci 20:1746–1753

Blau J, Young MW (1999) Cycling *Vrille* expression is required for a functional *Drosophila* clock. Cell 99:661–671

Ceriani MF, Hogenesch JB, Yanovsky M, Panda S, Straume M, Kay SA (2002) Genome-wide expression analysis in *Drosophila* reveals genes controlling circadian behavior. J Neurosci 22:9305–9319

Claridge-Chang A, Wijnen H, Naef F, Boothroyd C, Rajewsky N, Young MW (2001) Circadian regulation of gene expression systems in the *Drosophila* head. Neuron 32:657–671

Cyran SA, Buchsbaum AM, Reddy KL, Lin MC, Glossop NR, Hardin PE, Young MW, Storti RV, Blau J (2003) *vrille*, *Pdp1* and *dClock*
form a second feed back loop in the *Drosophila* circadian clock. Cell 112:329–341

Darlington TK, Wagner-Smith K, Ceriani MF, Staknis D, Gekasis N, Steeves TDL, Weitz CJ, Takahashi JS, Key SA (1998) Closing the circadian loop: clock-induce transcription of its own inhibitors *per* and *tim*. Science 280:1599–1603

Ewer J, Frisch B, Hamblen-Coyle MJ, Rosbash M, Hall JC (1992) Expression of the *period* clock gene within different cell types in the brain of *Drosophila* adults and mosaic analysis of these cells influence on circadian behavioral rhythms. J Neurosci 12:3321–3349

Frisch B, Hardin PE, Hamblen-Coyle MJ, Rosbash M, Hall JC (1994) A promoterless *period* gene mediates behavioral rhythmicity and cyclical per expression in a restricted subset of the *Drosophila* nervous system. Neuron 12:555–570

Frisch B, Fleissner G, Brandes C, Hall JC (1996) Staining in the brain of *Pachymorpha sexguttata* mediated by an antibody against a *Drosophila* clock-gene product: labeling of cells with possible importance for the beetle's circadian rhythms. Cell Tissue Res 286:411–429

Glossop NR, Houl JH, Zheng H, Ng FS, Dudek SM, Hardin PE (2003) VRILLE feeds back to control circadian transcription of clock in the *Drosophila* circadian oscillator. Neuron 37:249–261

Hardin PE (2004) Transcription regulation within the circadian clock: the E-box and beyond. J Biol Rhythms 19:348–360

Hardin PE, Hall JC, Rosbash M (1992) Behavioral and molecular analysis suggests that circadian output is disrupted by disconnected mutants in *D. melanogaster*. EMBO J 11:1–6

Helfrich-Förster C (1998) Robust circadian rhythmicity of *Drosophila melanogaster* requires the presence of lateral neurons: a brain-behavioral study of *disconnected* mutants. J Comp Physiol [A] 182:435–453

Helfrich-Förster C (2004) The circadian clock in the brain: a structural and functional comparison between mammals and insects. J Comp Physiol [A] 190:601–613

Helfrich-Förster C (2005) Organization of endogenous clocks in insects. Biochem Soc Trans 33:957–961

Houl JH, Yu W, Dudek SM, Hardin PE (2006) *Drosophila* CLOCK is constitutively expressed in circadian oscillator and non-oscillator cells. J Biol Rhythms 21:93–103

Lee C, Bae K, Edery I (1998) The *Drosophila* CLOCK protein undergoes daily rhythms in abundance, phosphorylation, and interactions with PER-TIM complex. Neuron 21:857–867

Markova EP, Shimada T, Takeda M (2003b) Daily expression patterns of *cycle* and *clock* genes in the head of the silkworm, *Bombyx mori*. J Biotech Biotechnol Equip 18:77–81

McDonald MJ, Rosbash M (2001) Microarray analysis and organization of circadian gene expression in *Drosophila*. Cell 107:567–578

Nishiitsutsuji-Uwo J, Pittendrigh CS (1968) Central nervous system control of circadian rhythmicity in the cockroach. II. The pathway of light signals that entrain the rhythm. Z Vergl Physiol 58:1–13

Renn SC, Park JH, Rosbash M, Hall JC, Taghert PH (1999) A *pdf* neuropeptide gene mutation and ablation of PDF neurons each cause severe abnormalities of behavioral circadian rhythms in *Drosophila*. Cell 99:791–802

Rutila JE, Suri V, Le M, So WV, Rosbash M, Hall JC (1998) CYCLE is a second bHLH-PAS clock protein essential for circadian rhythmicity and transcription of *Drosophila period* and *timeless*. Cell 93:805–814

Sauman I, Reppert SM (1996) Circadian clock neurons in the silkmoth *Antheraea pernyi*: novel mechanisms of Period protein regulation. Neuron 17:889–900

Schneider NL, Stengl M (2005) Pigment-dispersing factor and GABA synchronize cells of the isolated circadian clock of the cockroach *Leucophaea maderae*. J Neurosci 25:5138–5147

Sehadová H, Markova EP, Sehnal F, Takeda M (2004) Distribution of circadian clock-related proteins in the cephalic nervous system of the silkworm, *Bombyx mori*. J Biol Rhythms 19:466–482

Sehadová H, Shao QM, Sehnal F, Takeda M (2007) Neurohormones as putative circadian clock output signals in the central nervous system of two cricket species. Cell Tissue Res 328:239–255

Shao QM, Sehadová H, Ichihara N, Sehnal F, Takeda M (2006) Immunoreactivities to three circadian clock proteins in two ground crickets suggest interspecific diversity of the circadian clock structure. J Biol Rhythms 21:118–131

Shimizu T, Masaki S (1997) Geographical and species variation in circadian rhythm parameters in nemobiine crickets. Physiol Entomol 22:83–93

Sokolove PG (1975) Localization of the cockroach optic lobe circadian pacemaker with microlesions. Brain Res 87:13–21

Tomioka K, Chiba Y (1984) Effects of nymphal stage optic nerve severance of optic lobe removal on the circadian rhythm of the cricket, *Gryllus bimaculatus*. Zool Sci 1:385–394

Tomioka K, Abdelsalam S (2004) Circadian organization in hemimetabolous insects. Zool Sci 21:1153–1162

Ueda HR, Matsumoto A, Kawamura M, Iino M, Tanimura T, Hashimoto S (2002) Genome-wide transcriptional orchestration of circadian rhythm in *Drosophila*. J Biol Chem 277:14048–14052

Wang GK, Ousley A, Darlington TK, Chen D, Chen Y, Fu W, Hickman LJ, Kay SA, Sehgal A (2001) Regulation of the cycling of *timeless* (*tim*) RNA. J Neurobiol 47:161–175

Wise S, Davis NT, Tyndale E, Noveral J, Folwell MG, Bedian V, Emery IF, Siwicki KK (2002) Neuroanatomical studies of period gene expression in the hawkmoth, *Manduca sexta*. J Comp Neurol 447:366–380

Závodská R, Sauman I, Sehnal F (2003a) Distribution of PER protein, pigment-dispersing hormone, prothoracicotropic hormone, and eclosion hormone in the cephalic nervous system of insects. J Biol Rhythms 18:106–122

Závodská R, Sauman I, Sehnal F (2003b) The cycling and distribution of PER-like antigen in relation to neurons recognized by the antisera to PTTH and EH in *Thermobia domestica*. Insect Biochem Mol Biol 33:1227–1238

Zhu H, Yuan Q, Briscoe AD, Froy O, Casselman A, Reppert SM (2005) The two CRYs of butterfly. Curr Biol 15:R953–R954